

# Impacts of Tie-Lines and Wind Generator Location on Small Signal Stability of a Power System

T.R. Ayodele\*<sup>‡</sup>, A.A. Jimoh\*, J.L Munda\*, J.T Agee\*

\*Department of Electrical Engineering, Tshwane University of Technology

tayodele2001@yahoo.com, JimohAA@tut.ac.za, MundaJL@tut.ac.za, AgeeJT@tut.ac.za

<sup>‡</sup>Corresponding Author; T.R. Ayodele, Department of Electrical Engineering, Tshwane University of Technology, Private Bag X680 Pretoria 0001, Staatsartillerie Road, Pretoria West, South Africa, +27735605380, tayodele2001@yahoo.com

*Received: 15.10.2012 Accepted: 21.11.2012*

**Abstract-** This paper analyses the impact of tie-lines connecting different areas of power system and the location of wind farms on the small signal stability of a power system. The analysis is conducted using Monte Carlo simulation via modal analysis. The random samples are generated from two-parameter Weibull distribution to obtain possible representation of wind speed needed for the generation of wind power using Latin hypercube sampling techniques. The sampling technique allows the usage of a small sample size, which helps in reducing the simulation cost without jeopardising the accuracy of the result. Different scenarios are created and the oscillatory modes are calculated for different operating condition. The changes in modal characteristic of the system due to different operating conditions are evaluated by observing the movement on the complex plane. The results of the modal analysis for each scenario are validated using time domain simulation. Some of the key results show that wind power can have either positive or negative impact on the oscillation of a power system depending on the location in which it is integrated into the power system. It is also found out that strengthening the weak tie-lines can greatly improve the inter-area mode. This paper is useful in the planning stage of wind power projects.

**Keywords-** Wind power, Tie-lines, Power systems, Small signal stability, Wind power location, Monte Carlo simulation.

## 1. Introduction

With the rapid integration of wind power into the grid, wind generators are unavoidably forming a part of the power systems. In the past, power generation was dominated by conventional synchronous generators. In recent years, power systems are subjected to large penetration of wind power from other generators mainly induction generators. Therefore, the system dynamics which have been determined by synchronous generators is now being subjected to drastic change due to infiltration of induction generators

Unlike the conventional generators, the electricity from wind turbines is highly variable and therefore difficult to dispatch as a result of the stochastic nature of its prime movers i.e. wind speeds [1]. Moreover, most wind resources are found very far from the city where access to strong grid is limited. The grid in this area is initially planned for unidirectional power flow [2]. Electricity from wind generators is mainly transmitted through weak and congested grid. Under these circumstances, wind power may have a

negative impact on the small signal stability (SSS) of a power system.

SSS problem occurs when there is an insufficient damping of system oscillations as a result of changes in the operating parameters of a power system [3]. Low frequency oscillations have been the main concern in interconnected power systems, especially, weak connected systems and large power transmission over a long distance [4]. Oscillatory modes can be classified into control modes and electromechanical (EM) modes. Control modes result from the control system such as power system exciter, governors etc. These kinds of modes are of less concern in power system stability study. EMs typically between 0.1-2 Hz are the rotor angle modes which must be adequately damped for small signal-secured power system. Based on the frequency, EMs can further be classified into inter-area modes (0.1-0.8Hz) and local modes (0.8-2Hz).

Literature shows that wind generators themselves do not contribute to EM oscillation [5-7] because they are connected

asynchronously to the grid [6]. But, large penetration of wind power may alter the dispatch of the synchronous generators and cause a change in the load flow distribution that can lead to changes in the damping performance of a power system. It can also interact with the synchronous machine to change the damping torque induced on their shaft. Different impacts of wind power on the power system have been studied in the past. Shi et al [8] studied the impact of wind power penetration on SSS of a power system using DFIG technology. The effects of different generator technologies on power system electromechanical oscillation was the focus in [9]. This paper aims to examine the influence of interconnected tie-lines and the location of wind generators on the oscillatory modes of a power system.

Probability method is adopted in order to take into account the uncertainty in the behaviour of wind power using Monte Carlo Simulation (MCS) via modal analysis. Random samples are generated from Weibull distribution using Latin Hypercube Sampling (LHS) technique to obtain possible representative of wind speed needed for wind power generation. LHS method helps to use a small sample size without jeopardising the accuracy of the result [10]. This in turn increases greatly the simulation time.

## 2. Basic Monte Carlo Simulation Techniques

MCS is a set of computer algorithms for solving various kinds of uncertainty problems. It basically involves three basic steps. First, a random number from a given probability distribution is generated. A mathematical model is then solved deterministically to obtain the quantities of interest and finally a statistical analysis is performed. The first two steps are repeated a finite number of times. Uncertainty analysis relating to MCS can be described by a function as given by equation (1) [11]

$$v = h(z) \quad (1)$$

where  $h$  represents the function that describes the behaviour of the model under study,  $z$  and  $v$  are the vector of input and output variables respectively which are given by equation (2).

$$\begin{aligned} z &= [z_1, z_2, \dots]^T \\ v &= [v_1, v_2, \dots]^T \end{aligned} \quad (2)$$

where  $T$  is the transpose of a matrix. The objective is to determine the probability density function of the output variable  $v$  from the known probability density function of the input variable  $z$  in a repeated simulation process. In reality  $h$ , can be a complex function. In this paper, the output variable  $v$  is the statistical information and distribution of the eigenvalues, right and left eigenvector, damping ratio and damping frequency. The input variable  $z$  includes intermittent real and reactive wind power injection.

Traditionally, Simple Random Sampling (SRS) is used to generate random numbers from the known distribution for the input variables needed in uncertainty analysis. The limitation of this sampling method is that large numbers of sample size are required to recreate the distribution of the input variable. This is time consuming and computationally expensive. A recent study by the authors shows that about 100 samples size using LHS is enough to produce a reasonable result for practical purpose in probabilistic small signal stability applications [10].

### 2.1. Latin Hypercube Sampling Techniques

LHS is a stratified sampling technique that offers an efficient way of sampling random variables from the entire distribution [12]. The technique can be summarized as follows:

Step 1: For a sample size  $G$ , a uniform distribution with the range  $[0,1]$  is divided into  $k$  non overlapping intervals of equivalent length, hence the length of each interval is given as  $1/k$ .

Step 2: One sample value is chosen from each interval by choosing the midpoint without replacement. Hence,  $G$  random numbers are generated

Step 3: The wind speed is then generated by inverting the cumulative distribution function of the uniform distribution to Weibull distribution.

## 3. Model of Wind Energy Conversion System

The wind speeds used for the generation of wind power are drawn from LHS using two-parameter Weibull distribution which can be expressed as (3).

$$f_W(v) = \frac{k}{c} \left(\frac{v}{c}\right)^{k-1} \exp\left[-\left(\frac{v}{c}\right)^k\right] \quad (3)$$

where  $f_W(v)$  is the probability of observing wind speed( $v$ ).

$k$  and  $c$  are the Weibull shape and scale parameters of the distribution respectively. The values of the parameters are provided in Table 3 in the appendix. For a pitch-controlled turbine, the active wind power generated can be represented by parabolic equation (4).

$$P_e(v_i) = \begin{cases} P_r \frac{v_i^2 - v_{ci}^2}{v_r^2 - v_{ci}^2} & (v_{ci} \leq v_i \leq v_r) \\ P_r & (v_r \leq v_i \leq v_{co}) \\ 0 & (v_i \leq v_{ci} \text{ and } v_i \geq v_{co}) \end{cases} \quad (4)$$

where  $v_i$  is the wind speed generated from Weibull distribution using LHS method and  $v_{ci}, v_r, v_{co}$  are the cut-

in, rated and cut-out wind speed respectively,  $P_r$  is the rated wind turbine power. In this paper, the parameters of actual wind turbine (VESTAS-V82) are used for the simulation and are provided in Table 4 in the appendix. The reactive power generated can be derived from the equivalent circuit diagram of the induction generator as (5). The detailed model can be found in [13].

$$Q_{(vi)} = \frac{s_i^2 X(X + X_m) + r_2^2}{s_i X_m^2} P_{e(vi)} \tag{5}$$

where  $s_i$  is the rotor slip,  $x_1$  is the stator reactance,  $x_2$  is the rotor reactance,  $x_m$  is the magnetizing reactance,  $r_2$  is the rotor resistance and  $X = X_1 + X_2$ . The parameters of the asynchronous generator used are given in Table 5.

**4. Model of Wind Farm**

Combination of several Wind Energy Conversion Systems (WECSs) constitutes a Wind Farm (WF) which may be of the same types or different type of wind turbines. In this study, the WF is assumed to consist of the same types of wind turbines. For a WF with  $N$  identical numbers of wind turbines, the output power of the WF ( $P_{e(v_i)wf}$ ) at different wind speeds ( $v_i$ ) is given as (6)

$$P_{e(v_i)wf} = NP_{e(vi)} \tag{6}$$

Similarly, the reactive power absorbed by the wind farm can be expressed as (7).

$$Q_{(v_i)wf} = NQ_{(vi)} \tag{7}$$

**4.1. Power System Model and Small Signal Stability**

The dynamic behaviour of a non linear system such as a power system can be represented by equation (8)

$$\begin{aligned} \dot{x} &= f(x,u,t) \\ y &= g(x,u,t) \end{aligned} \tag{8}$$

Where

$$\begin{aligned} x &= (x_1, x_2, \dots, x_n)^T \\ u &= (u_1, u_2, \dots, u_n)^T \end{aligned}$$

$x$  is the state vector,  $u$  is the input vector,  $y$  is the output vector and  $T$  is the transpose. Linearising at the system equilibrium point will result in equation (9)

$$\begin{aligned} \Delta \dot{x} &= A \Delta x + B \Delta u \\ \Delta y &= C \Delta x + D \Delta u \end{aligned} \tag{9}$$

Subsequently, the system stability subject to small disturbance is studied based on the state matrix  $A$  as written in (10)

$$\det(\lambda I - A) = 0 \tag{10}$$

The values of  $\lambda$  that satisfy equation (10) are the eigenvalues of matrix  $A$ . They contain information about the response of the system to a small perturbation. The eigenvalue can be real and/or complex equation (11). The complex values appear in conjugate pairs if  $A$  is real.

$$\lambda_i = \sigma_i \pm j\omega_i \tag{11}$$

The frequency of oscillation in Hz and the damping ratio are given by equations. (12) and (13) respectively.

$$f = \frac{\omega_i}{2\pi} \tag{12}$$

$$\xi = \frac{-\sigma_i}{\sqrt{\sigma_i^2 + \omega_i^2}} \tag{13}$$

**5. System under Study**

An IEEE two area network as shown in Fig 1 is used for the study because it consists of two areas interconnected by weak tie lines. The network is slightly modified by connecting WF to bus 20 and later shifted to bus 120. This is to allow us compared the influence of wind generator location on the small signal stability of a power system. The system consists of four conventional synchronous generators and two nodal loads connected to bus 4 and 14. All the synchronous generators are described as 4th order and are equipped with IEEE type 1 exciter model. Power system stabiliser (PSS), prime mover and turbine governor are ignored. The parameters of the synchronous generator are provided in Table 6 in the appendix.

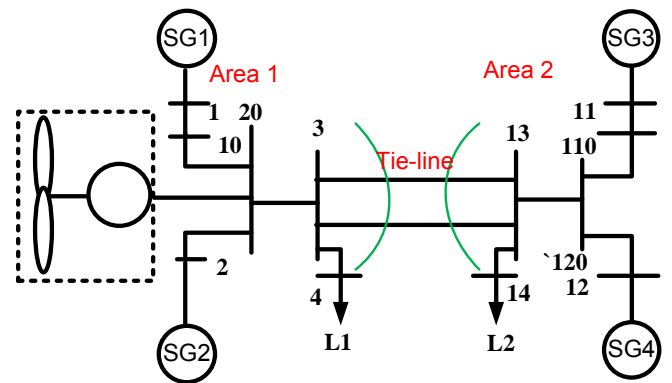


**Fig. 1.** IEEE 2-area network

The MCS algorithm for the analysis of small signal stability begins with the modelling of the input variables. The load flow analysis is carried out next using Newton Raphson algorithm, followed by the damping ratio computation via modal analysis. Finally, the results are analysed statistically. The flowchart of the proposed method is depicted in Fig. 2 and is programmed based on power system toolbox (PST) [14] in MATLAB.

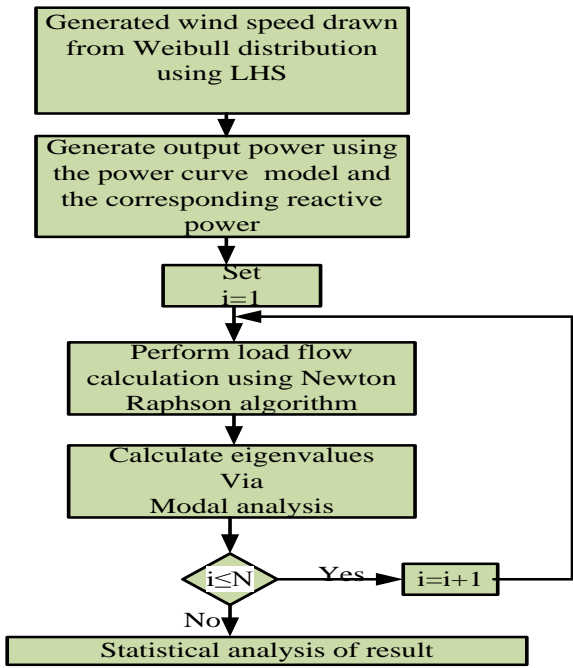


Fig. 2. The flowchart of MCS based small signal stability

The impact of wind power on small signal stability is studied under four scenarios (I-IV) and the results are discussed in section 6.

- a) Scenario I (base case): This include original network without wind farm. This consists of four synchronous generators only with the generators in area 1 interconnected by weak tie-lines to generators in area 2.
- b) Scenario II (WF is connected to bus 20): The WF consisting of 100 Wind Turbines (WTs) each of 1.65MW (total of 165MW) is connected to bus 20 in Fig 1.
- c) Scenario III (the weak tie line is strengthened): The tie-line between buses 3 and 13 in scenario II is strengthened by adding another tie-line between the two buses.

- d) Scenario IV (Location of WF changed to bus 120): The location of WF in scenario III is now shifted to bus 120. The wind power penetration when WF is connected this buses is then increased by increasing the WTs in the WF to 200, 300, 400 and 500 WTs. This means that the total power of the WF is increased from 165MW to 330, 495, 660 and 825MW respectively. The stability of the power system when the WF is located on bus 120 is compared to that of bus 20.

6. Result and Discussion

6.1. Scenario 1 (base case)

A total of 35 eigenvalues were obtained after solving the load flow and performing the modal analysis of the system. There were 18 oscillatory modes (9 conjugate pairs) of which 6 (3 conjugate pairs) are electromechanical modes. The results of the oscillatory modes are presented in Table 1. However, the interest lies in the electromechanical modes, which are the rotor angle modes that cause small signal instability in the power system if not properly damped. Electromechanical modes comprise two types: the inter-area modes and the local modes. The inter area modes are those that are excited as a result of a group of generators in an area swinging against the group of generators in another area, i.e. SG1 and SG2 in area 1 oscillating against SG3 and SG4 in area 2. Local modes involve a group of generators in the same area swinging against each other. Having solved the load flow and then calculated the eigenvalues and the eigenvectors, the IEEE 4-machine two area network was found to have one conjugate pair of inter-area modes (mode 7 & 8) and two conjugate pairs of local modes (modes 9 & 10 and 11 & 12). The eigenvalue, damping ratio and the oscillatory frequency of these modes are depicted in Table 1. All the modes were positively damped except the inter-area modes which have negative damping.

Table 1. Oscillatory mode in scenario I

**Table 1: Oscillatory mode in scenario I**

Modes	Eigenvalue	$\xi$	$f$	Type of modes
7&8	$0.05 \pm 3.90i$	-0.01	0.62	Inter area mode
9&10	$-0.60 \pm 7.25i$	0.08	1.15	Area 2 local mode
11&12	$-0.57 \pm 7.35i$	0.08	1.17	Area 1 local mode
13 &14	$-8.20 \pm 9.44i$	0.66	1.50	Control mode
15&16	$-8.02 \pm 9.84i$	0.63	1.57	Control mode
17± 18	$-5.4 \pm 15.10i$	0.34	2.40	Control mode
19&20	$-3.61 \pm 17.3i$	0.20	2.77	Control mode
24& 25	$-37.26 \pm 2.94$	1.0	0.47	Control mode
31&32	$-98.36 \pm 2.16$	1.0	0.34	Control mode

This signifies that the system is small signal unstable. The inter-area mode determines the stability of the entire system. The plot of real and imaginary parts in the complex plane is illustrated in Fig 3.

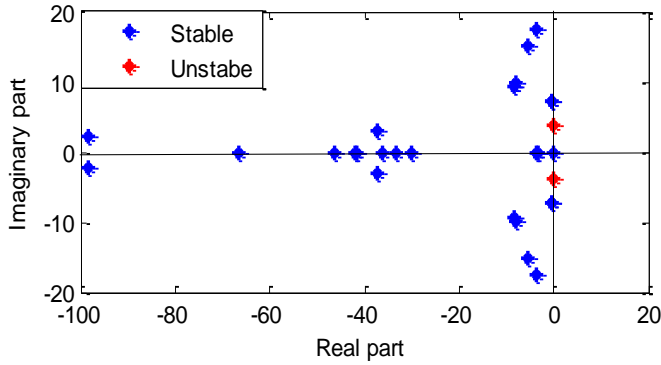


Fig. 3. Real and imaginary eigenvalue (scenario I)

The result of the modal analysis was verified using a time domain simulation by creating a three phase fault of duration 0.01s at the middle of the line connecting buses 3 and 13 at 1s. The result of both the speed and electrical power of the synchronous generators are presented in Fig. 4. The swinging between synchronous generators in area 1 (SG1 and SG2) and the one in area 2 (SG3 and SG4) are vividly evident in the figure. The oscillation between these two groups of generators increased following the fault until stability was lost. The instability was mainly due to the negatively damped inter-area mode, which was excited by the fault.

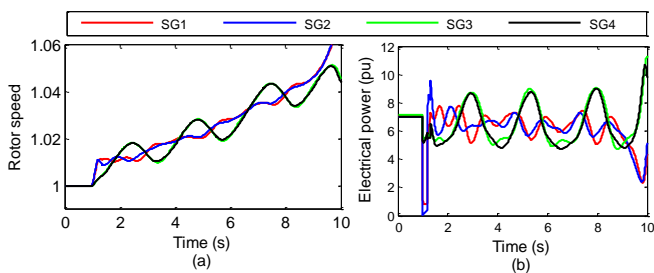


Fig. 4. The time domain simulation plot of (a) Rotor speed of the synchronous generators, and (b) The electrical output power of the synchronous generators.

The speed participation and the rotor angle plot of the generators involved in the inter-area mode are depicted in Fig. 5. The rotor angle plot in Fig 5b indicates that the oscillation of generators in area 1 and the one in area 2 are in the order of 1800. This is a confirmation that modes 7 and 8 are inter-area modes. It is evident in Fig 5a that SG3 has the highest participation value. This is the generator in which the power system stabiliser has to be installed in order to provide the most effective damping of the inter-area mode.

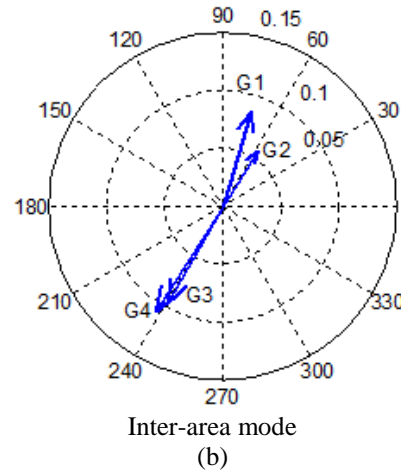
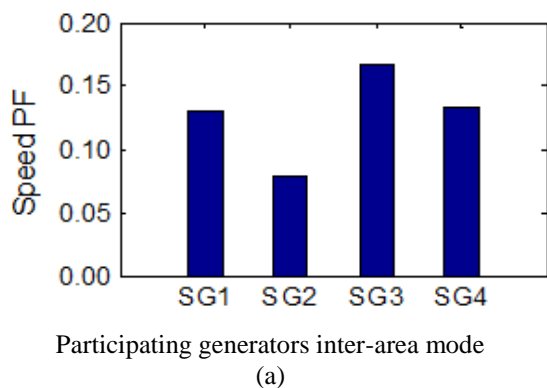


Fig. 5. The plot of (a) normalised speed bar plot of the participating generators in the inter-area mode, and (b) the rotor angle compass plot of the inter-area mode

6.2. Scenario II (Wind farm connected to bus 20)

A WF consisting of 100 WTs each of rated power of 1.65MW was connected to bus 20. After solving the load flow and calculating the eigenvalues, a total of 35 eigenvalues were obtained. This signifies that no additional modes are added or subtracted from scenario I. The results of the mean damping ratio and mean frequency when a WF consisting of 100 WTs (165MW) is connected to bus 20 are presented in Table 2. The results in the table indicate that the damping ratio of the inter area modes decreased from -0.01 to -0.0159. It is evident that the connection of the WF to the system at bus 20 affected the damping of the inter-area and area 1 local mode negatively. The area 2 local mode remains unaffected.

Table 2. Electromechanical modes with wind farm connected to bus 20

EM modes	$E(\xi)$	$\sigma(\xi)$	$E(f)$	$\sigma(\xi)$
7&8 (Inter-area mode)	-0.0159	0.0036	0.620	$4.97 \times 10^{-4}$
9 & 10 (Area 2 local mode)	0.0828	$1.6 \times 10^{-4}$	1.155	$7.52 \times 10^{-4}$
11&12 (Area 1 local mode)	0.0691	0.0080	1.173	0.0023

6.3. Scenario III (The weak tie line is strengthened with wind farm connected to bus 20)

The network in scenario II was restructured so that an additional tie-line was added to the two area network between bus 3 and 13. After solving the load flow and perform the modal analysis of the system, all the modes have damping ratio greater than 5%. This indicates that the new network is strongly damped. This is because the weak tie-line in the original network had been reinforced. It can be concluded that strengthening the weak tie-line interconnecting different areas of a power system can improve the overall damping of the system. Figure 6 depicts the plot of the real part versus the imaginary part of the eigenvalues of the strengthened network in the complex

plane and the plot of the damping ratio versus the frequency. The figures indicate that all the oscillatory modes have a damping ratio greater than 5%. The results of the modal analysis in Fig 6 were validated using time domain simulation and the result is presented in Fig 7. The

simulation results shows that after a three phase fault of 0.01s was created at 1 s, the oscillation in the speed and output power of the synchronous generators died out very quickly, signifying a strongly damped system.

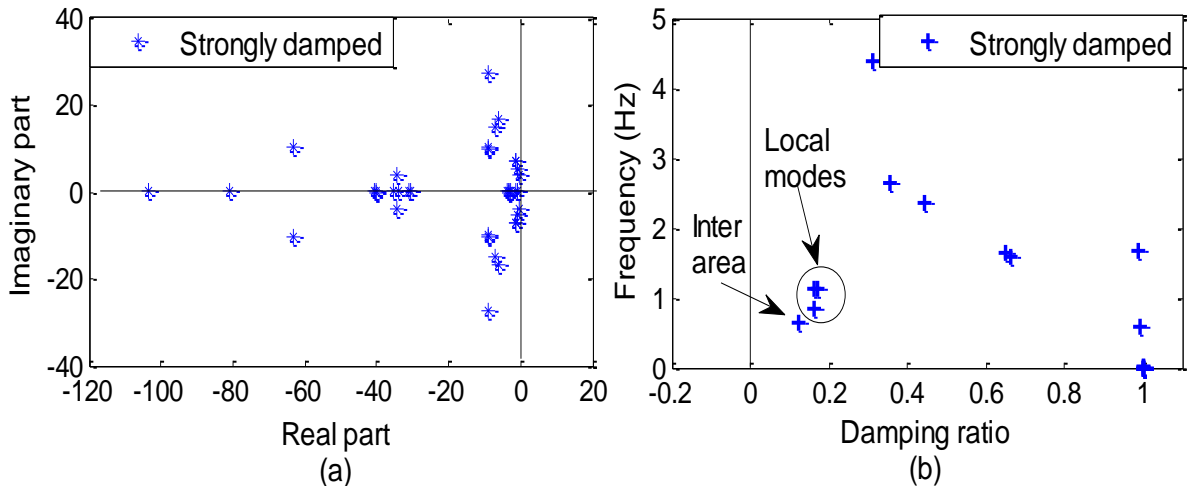


Fig. 6. The plot of (a) Real part versus imaginary part of eigenvalues (b) Damping ratio versus frequency

6.4. Scenario IV (The location of WF changed to bus 120)

The location of the WF in scenario III was shifted from bus 20 to bus 120. The wind power penetration at this bus is increased by increasing the numbers of WTs to 200, 300, 400 and 500 WTs respectively. For the entire operating scenario, the simulation results show that the mean damping ratios of all the eigenvalues are greater than 5%. All the modes are

strongly damped at all the operating conditions. The results of the inter-area mode of the system when WF was connected to bus 20 and then shifted to bus 120 at increasing wind power penetration are presented in Fig 8 and Fig. 9, respectively. The results in the figures demonstrate that the damping reduced as the wind power penetration increased when the WF was connected to bus 20. However, when the wind farm was shifted to bus 120, the damping increased as the wind power penetration increased.

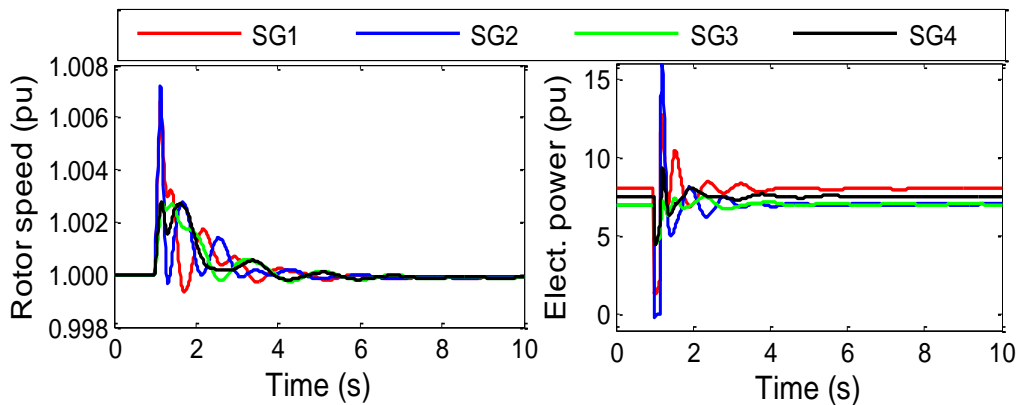


Fig. 7. The plots of (a) Rotor angle of the generators contributing to the inter-area mode, and (b) Electrical power output of the generators in the restructured IEEE network

It can be inferred that the wind generators can improve or reduce the system damping depending on the location in which it is connected to power system. The results of the modal analysis with respect to WF location were validated by creating a three phase fault of duration 0.01s at 1s on the line connecting bus 3 and bus 13 in the restructured (strengthened) network. Both the speed and the electrical power of the synchronous generators 2 and 4 (SG2 and SG4) were observed. The results are presented in Fig 10 and Fig 11, respectively. The figures indicate that both the speed and the electrical power of the synchronous generators were

better damped when the WF was connected to bus 120 compared to bus 20.

7. Conclusion

In this paper, the impact of intermittent wind power on power system oscillation has been studied. It was demonstrated that the impacts of wind power on the damping can be positive or negative depending on the wind power integration and the location. Connection of wind generator to bus 120 improves the inter-area mode compared to bus 20. It

was also demonstrated that strengthening of weak tie-lines interconnecting different areas of power system can greatly improve the damping of a power system consisting of

intermittent wind generation. Although, the construction of new lines is capital intensive, it may be unavoidable if this becomes necessary.

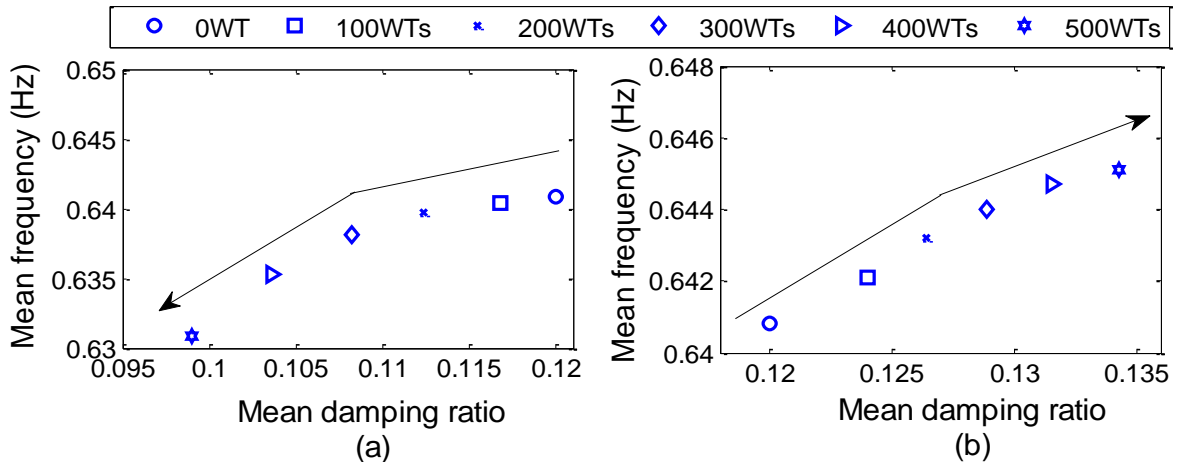


**Fig. 8.** The plots of mean damping ratio versus mean frequency of the inter-area mode when WF is connected to (a) bus 20 (b) bus 120 at different penetration level

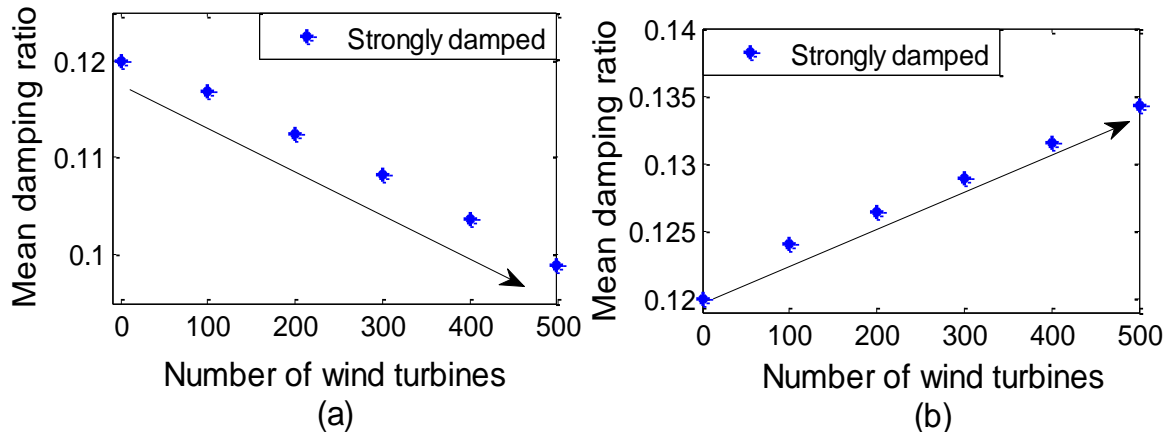


**Fig. 9.** The plots of mean damping ratio versus wind power penetration (Numbers of wind turbines) at (a) bus 20 (b) bus 120

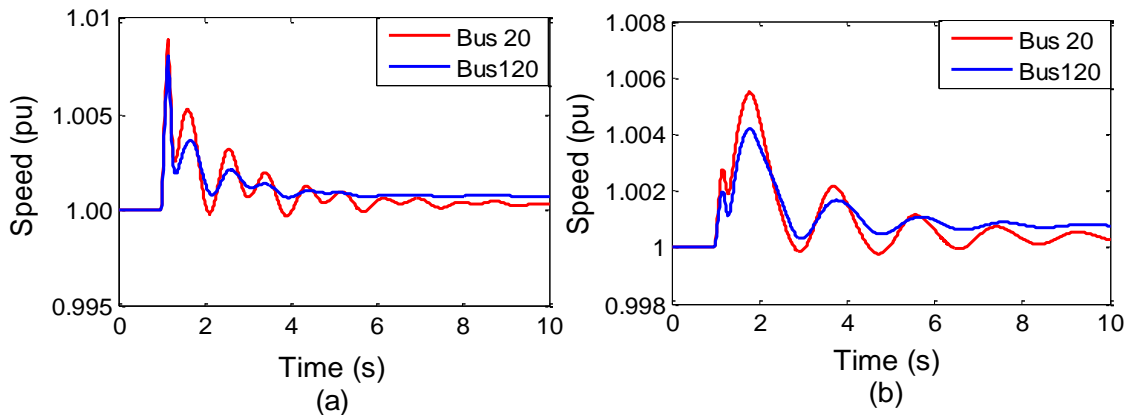


**Fig. 10.** The time domain speed plots of (a) SG2 (b) SG4 when WF is connected to bus 20 and bus 120

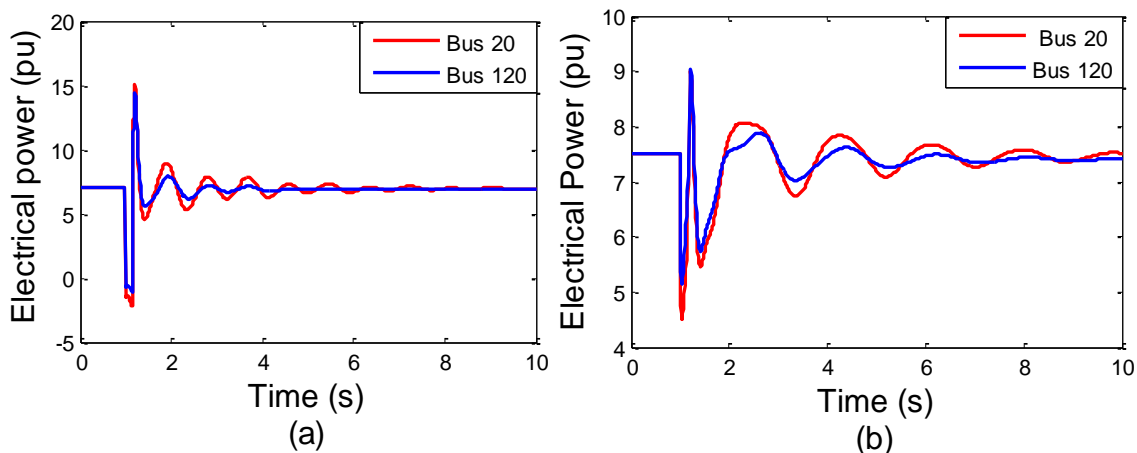


**Fig. 11.** The time domain electrical power plots of (a) SG2 (b) SG4 when WF is connected to bus 20 and bus 120

**Acknowledgements**

The Authors would like to thank the Tshwane University of Technology for the financial support of the research

**References**

[1] G. Papaefthymiou, et al., "Integration of stochastic generation in power systems," *International Journal of Electrical Power & Energy Systems*, vol. 28, pp. 655-667, 2006.

[2] T. R. Ayodele, et al., "The Challenges of Integrating Intermittent Renewable Energy sources on the Power System grid Integrity:A review," presented at the 1st International Conference on Green and Sustainable Technology: Research and Workforce Development, Greensboro, North Carolina, USA, 2010.

[3] P. Kundur, *Power System Stability and Control*, The EPRI Power System Engineering Series vol. 1: McGraw-Hill, Inc, New York, 1994.

[4] A. Mendonca and J. A. P. Lopes, "Impact of large scale wind power integration on small signal stability," in *International Conference on Future Power Systems*, Amsterdam, 2005, pp. 5 pp.-5.

[5] J. G. Slootweg and W. L. Kling, "The Impact of Wind Power Generation on Power System Oscillations," *Electric Power System Research*, vol. 67, pp. 9-20, 2003.

[6] D. J. Vowles, et al., "Effect of wind generation on small-signal stability ; A New Zealand Example," in *Power and Energy Society General Meeting - Conversion and Delivery of Electrical Energy in the 21st Century*, 2008 IEEE, Pittsburgh, Pennsylvania, USA, 2008, pp. 1-8.

[7] J. Stenzel, et al., "Impact of Large Scale Wind Power on Power System Stability," in *5th International Workshop on Large-Scale Integration of Wind and Transmission Network for Offshore Wind Farm.*, Glasgow, Scotland, 2005.

[8] L. B. Shi, et al., "Analysis of Impacts of Grid-Connected Wind Power on Small Signal Stability," *Wind Energy* (Wiley online), 2010.

[9] S. Ghosh and N. Senroy, "Effect of generator type on the participation of adjacent synchronous machines in electromechanical oscillations," in *Joint International Conference on Power Electronics, Drives and Energy Systems (PEDES) India*, 2010, pp. 1-3.

[10] T. R. Ayodele, et al., "Performance Evaluation of Sampling Techniques in Monte Carlo Simulation-Based Probabilistic Small Signal Stability Ananalysis," presented at the *The 23rd IASTED International Conference on Modelling and Simulation (MS 2012)*, Banff, Canada, 2012.

[11] H. Yu, et al., "Probabilistic Load Flow Evaluation With Hybrid Latin Hypercube Sampling and Cholesky Decomposition," *IEEE Transaction on Power Systems*, vol. 24, 2009.

[12] J. C. Helton and F. J. Davis, "Latin Hypercube Sampling and the Propagation of Uncertainty in Analysis of Complex System," *Reliability Engineering & System Safety*, vol. 81, pp. 23-69, 2003.

[13] T. R. Ayodele, et al., "Probabilistic Small Signal Stability Analysis of a Power System Consisting Intermittent Wind Generation " in *12th International conference on Probabilistic Methods Applied to Power System*, Istanbul, Turkey, 2012.

[14] J. Chow, "Power System Toolbox 2.0- Dynamic Tutoria and Functions," *Cherry Tree Scientific Software*, 2000.

**Appendix**

**Table 3.** Wind distribution parameters

Parameters	Values
Shape, ( $k$ )	2.24
Scale, ( $c$ )	7.61m/s

**Table 4.** VESTAS-V82 Wind turbine parameters

Wind Turbine (VESTAS-V82)	Parameters
Rated Power (kW)	1650
Hub height (m)	70
$\eta_t$ overall efficiency (%)	95
Cut-in wind speed ( $v_{ci}$ ) (m/s)	3
Rated wind speed ( $v_r$ ) (m/s)	13
Cut-out speed ( $v_{co}$ ) (m/s)	20

**Table 5.** Induction generator parameters

Asynchronous generator	Parameters
Rotor resistance $r_2$ (pu)	0.009
Stator reactance $X_1$ (pu)	0.01
Rotor reactance $X_2$ (pu)	0.01
Magnetising reactance $X_m$ (pu)	3.0
Inertia (H) (s)	2